Relationships between lower and upper crust tectonic during doming: the mylonitic southern edge of the Velay metamorphic core complex (Cévennes-French Massif Central)

Pierre Bouilhol, André François Leyreloup, Claude Delor, Alain Vauchez, Patrick Monié

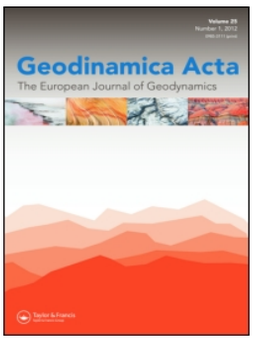

Geodinamica Acta

ISSN: 0985-3111 (Print) 1778-3593 (Online) Journal homepage: https://www.tandfonline.com/loi/tgda20

Relationships between lower and upper crust tectonic during doming: the mylonitic southern edge of the Velay metamorphic core complex (Cévennes-French Massif Central)

Pierre Bouilhol , André François Leyreloup , Claude Delor , Alain Vauchez & Patrick Monié

To cite this article: Pierre Bouilhol , André François Leyreloup , Claude Delor , Alain Vauchez & Patrick Monié (2006) Relationships between lower and upper crust tectonic during doming: the mylonitic southern edge of the Velay metamorphic core complex (Cévennes-French Massif Central), Geodinamica Acta, 19:3-4, 137-153, DOI: 10.3166/ga.19.137-153

To link to this article: https://doi.org/10.3166/ga.19.137-153

Geodinamica Acta

Geodinamica Acta 19/3-4 (2006) 137-153

Relationships between lower and upper crust tectonic during doming: the mylonitic southern edge of the Velay metamorphic core complex (Cévennes-French Massif Central)

Pierre Bouilhol [a]*, André François Leyreloup [b], Claude Delor [c], Alain Vauchez [d], Patrick Monié [e]

[a] *Laboratoire Dynamique de la Lithosphère, équipe géochimie, Université Montpellier II, France.*
Now at: ETH Structuralgeology, Leonhardstrasse 19, LEB D10, 8092-Zurich, Switzerland
[b] *Laboratoire Dynamique de la Lithosphère, équipe géochimie, Université Montpellier II, France*
[c] *BRGM, Orléans, France*
[d] *Laboratoire de Tectonophysique, Université Montpellier II, France*
[e] *Laboratoire Dynamique de la Lithosphère, équipe géochimie, Université Montpellier II, France*

Received: 13/02/06, accepted: 03/05/06

Abstract

Petrological, structural, and thermochronological analyses have been focused on the Mylonitic Metamorphic Vellave Zone (MMVZ), which wraps around the southern edge of the Velay metamorphic core complex dome. Mineral-stretching lineations in the Sil-Bt zone are everywhere perpendicular to the dome edge, the strong mylonitic foliation displays top-to-the south normal shearing, and preferential quartz orientations show high-temperature prismatic <a> deformation interpreted as pure shear patterns. The Sil-Bt zone reflects the dome dynamics during its forced emplacement and uplift. From the contact aureole of the Borne monzogranite, through greenschist facies, and until the And-Crd-Bt zone of the MMVZ, the series are affected by constant syn-metamorphic top-to-the-northeast shearing, acting since at least 320 Ma and reflecting upper crust tectonics during doming: the detachment system. A constriction-dominated deformation regime characterizes the And-Crd-Bt zone, together with the fact that thermochronometers (micas Ar/Ar, U-Th/Pb monazite) are set at 310 Ma, reflecting fast cooling and uplift high in the crust, consequently, the MMVZ is a mylonite that represents the interaction of dome dynamics and the tectonic environment of the upper crust. The Velay dome was forcibly emplaced in the country rocks, and has intruded its own detachment, showing the relationship between the detachment and the dynamic of the dome on its southern edge.

Keywords: metamorphic core complex – HT mylonite – HT/LP metamorphism - Quartz CPO - $^{40}Ar/^{39}Ar$

1. Introduction

Metamorphic Core Complexes (MCCs) have been specially described in the hinterland of collapsed orogens. These regional-scale migmatitic bodies are regarded as illustrating the thinning of a thickened crust during post-collisional evolution. Their emplacement is commonly facilitated by an asymmetric detachment fault (e.g. [1] [2]) that permits the upwelling of deeper molten lower crust. Their exhumation is also linked to erosion processes that affect the relief generated during previous crustal thickening [3]. However, the real relationship between the detachment and the dome emplacement dynamic is still poorly known. The dynamics of MCC emplacement are still debated and further work is needed on the thermal and mechanical effects of MCC emplacement in order to increase our understanding of emplacement modes.

* Corresponding author.
Tel: +41 (0)44 63 28 213
E-mail address: pierre.bouilhol@erdw.ethz.ch

We present an example of the interaction between the emplacement dynamics of an MCC and its surroundings rocks. The Velay anatectic dome (French Massif Central) is a Hercynian MCC, emplaced in the hinterland of the collapsed Variscan orogen during its late evolution. The emplacement dynamics and P-T conditions of formation of this huge migmatite body (about 100 km in diameter) have been well documented with special reference to:

i. The northern 'Pilat' detachment fault [4];
ii. The southern expansion of the entire structure of the body [5, 6, 7];
iii. The discharge of the dome in the surrounding rocks on the southern edge, with overturning of the migmatitic structure [2, 8];
iv. The uplift of Grt-Crd-bearing migmatite [9, 10, 11].

All mineral abbreviations are from Kretz [12].

We studied the entire eastern Cévennes area, and our study focuses on the southern edge of the dome at the boundary between the dome and the schists in order to firstly, localize the mylonitic detachment zone in that region and, secondly, to decipher the part of the deformation due to the detachment and the part due to dome uplift. Finally, we propose a model for the evolution of the migmatitic Velay core complex that provides a better understanding of the relationships between dome dynamics and deformation of the upper crust governed by the detachment fault.

2. Geological setting

2.1. The place of the Velay dome in the collapsed Variscan orogeny

The French Variscan belt resulted from collision between Laurussia and Gondwana [e.g.13, 14, 15], leading to a thickened lithosphere of which the so-called Leptynite Amphibolite Group (LAG) represents the southward thrust suture onto the Gondwana margin (Fig. 1). From 330 to 290 Ma this collision evolved from a syn- into a post-orogenic regime, due to collapse of the belt [e.g. 16]. This late evolution stage is indicated by a HT-LP metamorphism that created granulitization of the lower crust [17]. Partial melting of the lower and middle crust then led to the emplacement of granitic (S and I type) magma and to the uplift of a migmatitic core complex in the foreland, the Montagne Noire massif [18] (Fig. 1) as well as of the Velay dome in the hinterland (e.g. [9]) (Figs. 1, 2). The Velay dome has overprinted the thickening structures; for example in the roof of the dome, the major abnormal contact (LAG: thrust suture) was digested by diatexites, but can still be found as a klippe [20] and in a pinched syncline on the east edge of the dome [21] (Figs. 1, 2). This implies that all medium- and supra-crustal metamorphic rocks of the thrust pile have been eroded [2].

This last major event marks the end of the Hercynian orogeny and has exposed the actual architecture of the belt.

2.1.1 Geology of the dome

The Velay dome is one of the largest migmatitic and granitic domes of the Variscan belt. Granite and migmatite genesis of the

Fig. 1: Geological map of the Massif Central (from [3], modified) with the location of high-pressure rocks, the Cévennes, the Velay dome, the Montagne Noire, and the corresponding section below. Note that the southern edge of the dome is overturned on the Cévennes area, and that it intrude eo-Hercynian structures (e.g. L.A.G).

dome are well documented [e.g. 22, 9, 23, 10, 11], describing a multistage granite emplacement during the dome's history. The dome has a concentric shape, with external orthogneiss (e.g. Tanargue on the southern edge and Arc de Fix on the western edge) and paragneiss metatexites intruded by Grt-Crd-bearing diatexites and nebulites, which then were intruded by Crd-bearing granites and dry leucogranites (e.g. Pont de Labaume on the southern edge). Because of this multi-intrusion history, the dome is regarded as a polydiapir. Two main metamorphic episodes – M3, M4 – leading to anatexis (following an uncertain M1 episode, and a HP M2 episode due to thickening) were described by Montel *et al.* [11]; M3 and M4 were low- to medium-P high-T metamorphism that both gave rise to Velay migmatites and granites from 340 to 300 Ma. M3 could correspond to emplacement of the dome and syntectonic granitoids, while the M4 event may have been more widespread leading to nebulites and post-anatectic granites. These events will be discussed in part 4.

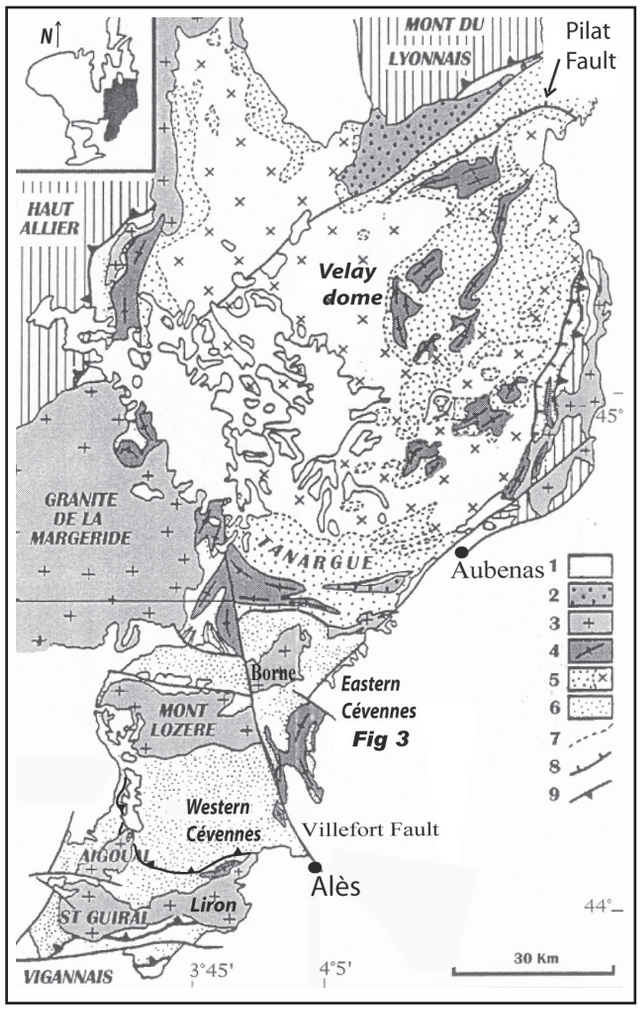

Fig. 2: Simplified Cévennes and Velay map with the location of the studied area (modified after [19];).

1: Post-Carboniferous basaltic and sedimentary covers. 2: Stephanian. 3: Granites. 4: Orthogneisses. 5: Velay anatectic gneisses and granites. 6: Paleozoic Cévennes micaschists. 7: Contact between granites and Velay Dome gneisses. 8: Ductile normal fault. 9: Principal thrusts

2.1.2. Model of emplacement and tectonic context of the dome

The major north-dipping Pilat detachment fault [4] (Fig. 2) explains the emplacement of the dome on its northern edge and gives us a key in understanding the emplacement dynamics. The work of Lagarde *et al*. [6, 7] provided a broader view of these dynamics by studying the entire body from a structural point of view; it highlights the wrench-tectonics context of the emplacement and the fact that the dome suffered southward expansion while the northern part was sheared along the Pilat fault (Figs. 1, 2). Normal northward-faulted klippen were also preserved on the northern roof of the dome, indicating that the dome intruded the detachment fault.

Burg and Vanderhaeghe [8], studying way-up criteria in migmatites of the southern edge, showed that the migmatitic structure is overturned to the south (due to migmatisation dynamics) onto the schists of the Cévennes area (Fig. 1). The southern dome edge is characterized by several kilometric folds in migmatized Tanargue para- and orthogneisses, with E-W axes and a tendency to be overturned to the north.

2.2. The Cévennes area

The Cévennes schists area (Figs. 1, 2) is regarded as the parautochthonous domain of the Variscan belt that formed the north-Gondwana margin during subduction [14]. The Cévennes can be divided in two parts, bounded by the sinistral Villefort wrench fault (Fig. 2). The slaty rocks are composed of azoic volcanoclastic graphitic schists and quartzites supposed to be Cambro-Ordovician in age [24], which underwent the thickening episode. The western domain is characterized by numerous intra-schist thrust faults, interpreted as representing a southward thrust complex developed during the thickening episode [25, 26]. The metasedimentary rocks have recorded a LP-HT metamorphism [26]. The metamorphic degree increases to the northeast toward the dome, where it reaches its climax. The Grt-in, Cld-out; St-And-Crd-in; Sil-in isograds reflect the Velay dome's shape and geometry, and are never parallel to the main thrust contact. The Grt-in isograde crosscuts intraschist phyllonites, which suggests that this metamorphism was due to the intrusion of the Velay Dome (320-310 Ma), resulting in a giant contact metamorphism, rather than to the thickening event. Note that Grt is present throughout the assemblage, from the Grt-in isograde until the dome (anatexis), and that the part of the foliation produced by the intrusion of the dome is still unknown.

The tectonometamorphic evolution of the eastern domain is still poorly understood: the metamorphic map of Marignac *et al*. [27] does not give an overview of the processes involved in the dome intrusion. The tectonic evolution described in [28, 29] does not always end with our conclusions. In any case, the thermal and mechanical effects of dome emplacement and its discharge in the schist domain [8] remain mostly unknown.

3. Data

3.1. Geology of the Eastern Cévennes

Our new geological map (Fig. 3) shows considerable differences with those of [29] and [30]. The eastern Cévennes are mostly composed of quartz-feldspar schist with some quartzite layers, an orthogneiss is exposed in the south (la Cézarenque gneiss), and black graphitic schist is found in a kilometre-size tectonic boudin bounded by two top-to-the-east normal faults (Fig. 3). These units are intruded by the Borne and Rocles granites and constitute the host rocks of the Velay dome.

The Borne granite, an I-type calc-alkaline monzogranite dated at 315 + 5 Ma (Rb/Sr whole rock, [31]), is the eastern part of the Mont Lozère pluton displaced northward along the Villefort fault. The Rocles granite is a composite S-type

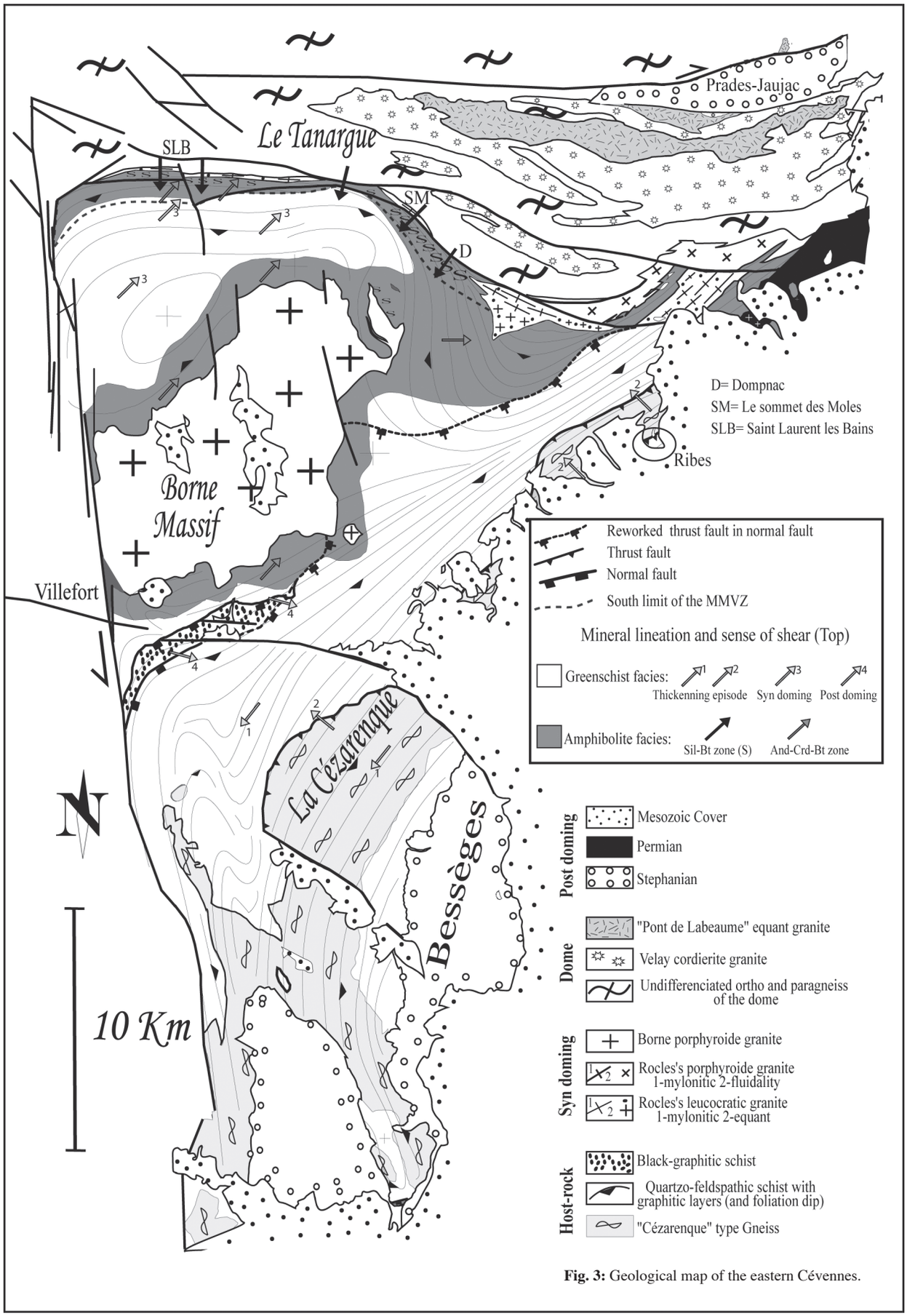

Fig. 3: Geological map of the eastern Cévennes.

leucogranite (318 + 3 Ma U-Th/Pb on monazite, [32]) (Fig. 3). Blasts from the metamorphic aureole of both granites include Bt, And and Crd, with locally Sil close to the contact with the granite. The fact that the two metamorphic aureoles coalesce at the northeast termination of the Borne granite suggests that their emplacement could be contemporaneous.

The mineralogy of both metamorphic aureoles is the same as the assemblage found in the regional metamorphism found in a mylonitic band wrapping the dome edge. Most schists are in the greenschist facies. Grt is generally associated with Chl, Ms and, rarely, with Bt, defining the Grt-Chl zone. Using Grambling [33] Grt-Chl thermometry, it appears that the metamorphic peak temperature never exceeded 500 °C. This greenschist facies can be inferred to relate to the intrusion of the Velay dome, as well as to the thickening one. However, as long as no modern metamorphic calibration and absolute age dating will be carried out on the greenschist facies rocks, it will remain difficult to distinguish the contribution of each of these episodes. Grt-St micaschists belonging to the Barrovian thickening metamorphism were noted in an outcrop in Ribes (Fig. 3) as a slice thrusted northwest onto the Cézarenque unit (this study, and e.g. [34]).

From a structural view point, we can distinguish four tectonic events (Fig. 3):

➤ The first one, proposed by previous authors (e.g. [28, 34, 35]), could be related to southward thrusting as observed in the western part [25] (but has never been characterized in this study).

➤ The second one is northwest thrusting which led to overthrusting of the Ribes Barrovian schists onto the Grt-Chl schists (Fig. 3). Top-to-the NW sense of shear is well preserved at the contact between Ribes's schists and the orthogneiss, where ductile criteria in the Cézarenque gneiss, and C/S structures in the Ribes schist attest of this movement. It seems that both thrusting events never created above-greenschist facies conditions.

➤ The third one corresponds to the tectonic regime during the intrusion of the Dome du Velay and is the subject of the study. This regime is caracterized by top-to-the NE sense of shear, and affects all the greenschist-facies rocks that correspond to the highest structural terrain of the area (between the Borne granite and the anatectic dome) but also the metamorphic aureole of the Borne granite (Fig. 3). The contact metamorphism of the Borne granite (310 + 3 Ma $^{40}Ar/^{39}Ar$ on Bt, [36]) was contemporaneous with top-to-the-northeast shearing (Fig.3) inducing a strong foliation and creating a primary aureole, that locally is overprinted by atectonic blasts. These new data, together with the NE-SW pluton geometry, indicate that the Borne is a laccolith emplaced during this tectonic event. This interpretation is not consistent with earlier work [28, 29, 37] that suggested emplacement during an E-W extensional regime (the fourth one reported below). This new interpretation needs to be tested with further work on the Borne granite itself, which was not the subject of this study.

➤ The Fourth one is characterized by E-W extension define by a normal fault (within the Grt-Chl zone), south of Borne granite. This extension is post granite emplacement as suggested by the presence of a Crd+Bt hornfels boudin and was contemporaneous with the formation of the Bessèges coal basin (Fig. 3).

The regional metamorphism is only exposed in a mylonitic contact which bounds the southern dome edge. This Metamorphic Mylonitic Vellave Zone, or MMVZ, never described before, runs from the Villefort fault to the Rocles granite (Fig. 3). The 700m-thick mylonitic foliation (south dipping) wraps around the dome and juxtaposes Cévennes greenschist against the anatectic dome. This mylonite affects various rocktypes and all metamorphic minerals are contemporaneous with the deformation observed in the MMVZ where two metamorphic zones are found:

➤ In the roof, And, Crd and Bt are index minerals (+Qtz+Ms+NaPl+polymorphic TiO_2+Zr+Mnz+Xe) in metapelites, defining a single LP-MT metamorphic zone, i.e. the And-Crd-Bt zone,

➤ Against the dome, Sil formed firstly from And, then Ms reacts with Qtz (Ms-out) to give Sil + Kfs + H_2O granulitic paragneiss (up to 30 meters thick) then evolving to anatectic biotitic paragneiss (Sil + Kfs + melt). This transition toward the Velay migmatites characterizes the sillimanite metamorphic zone, i.e. the Sil-Bt zone. This metamorphic succession defines a typical LP gradient (2-3.5 Kbar).

Contact between the Sil-Bt zone and the metatectitic Tanargue orthogneiss is marked by a 20m-thick unit where mylonitic meta-granite and leucosomes from anatexis of metapelites coexist intimately and show Sil bearing shear bands.

In the eastern part of the MMVZ, mylonitic foliation begins in the greenschist facies and moves toward the Sil-Bt zone to the west, reflecting deeper level exposition toward Rocles granite. This area displays a particular relationship between the anatectic dome and the Cévennes area host rocks.

3.2. The Mylonitic Metamorphic Vellave Zone (MMVZ)

3.2.1. Petrostructural analysis

This section describes the main petrostructural characteristics of each metamorphic zone of the MMVZ with their special features. The characteristics are derived from three detailed cross sections: St Laurent-les-Bains (SLB), Le Sommet des Moles (SM), and Dompnac (D) (Figs. 3 and 4).

The Sillimanite zone (Sil-Bt zone)

This zone displays very strong mylonitic foliation, dipping south (between 30° and 50°) and wrapping around the dome edge. Mineral stretching lineation is everywhere perpendicular to the dome edge, in the dip of the foliation. It is characterized by oriented Sil fibres as well as by ellipsoidal Bt aggregates. The Sil formed around And blasts and also replaces Bt, defining the Sil+ isograde. In the eastern part (SM and D) the Sil-Bt zone affects mostly a quartzite with thin layers of more pelitic layers, whereas black schist dominates in SLB. At a macroscopic scale, shear-sense criteria are rare, especially in the eastern part on the Dompnac

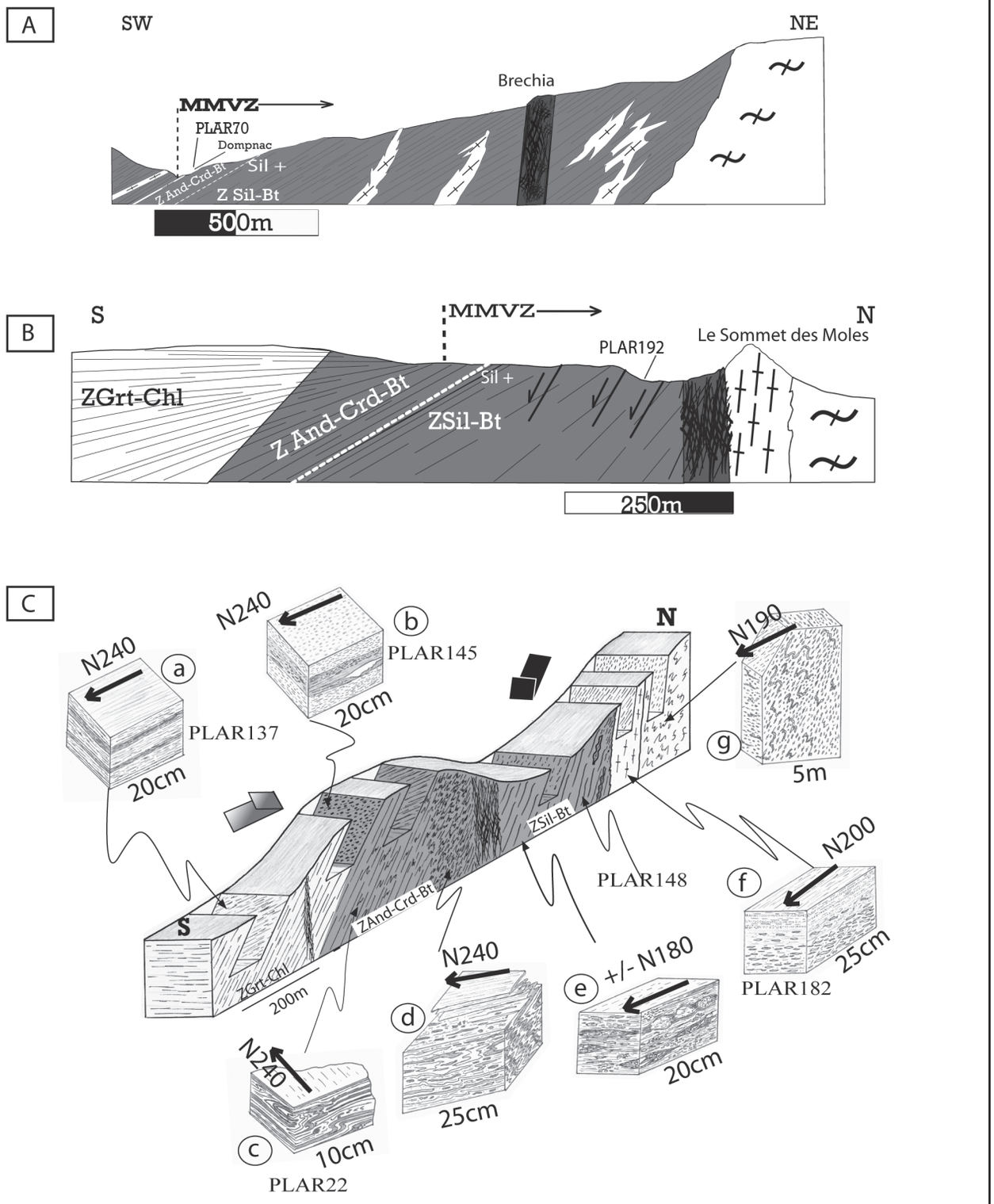

Fig. 4: The three main cross sections: A: Dompnac (D) cross section; B: Sommet des Moles (SM) cross section; C: Saint Laurent-les-Bains (SLB) block diagram of the cross section; a, b, c, d, e, f represent samples from the cross section. Legends and locations of the cross sections are the same as in Fig. 3.

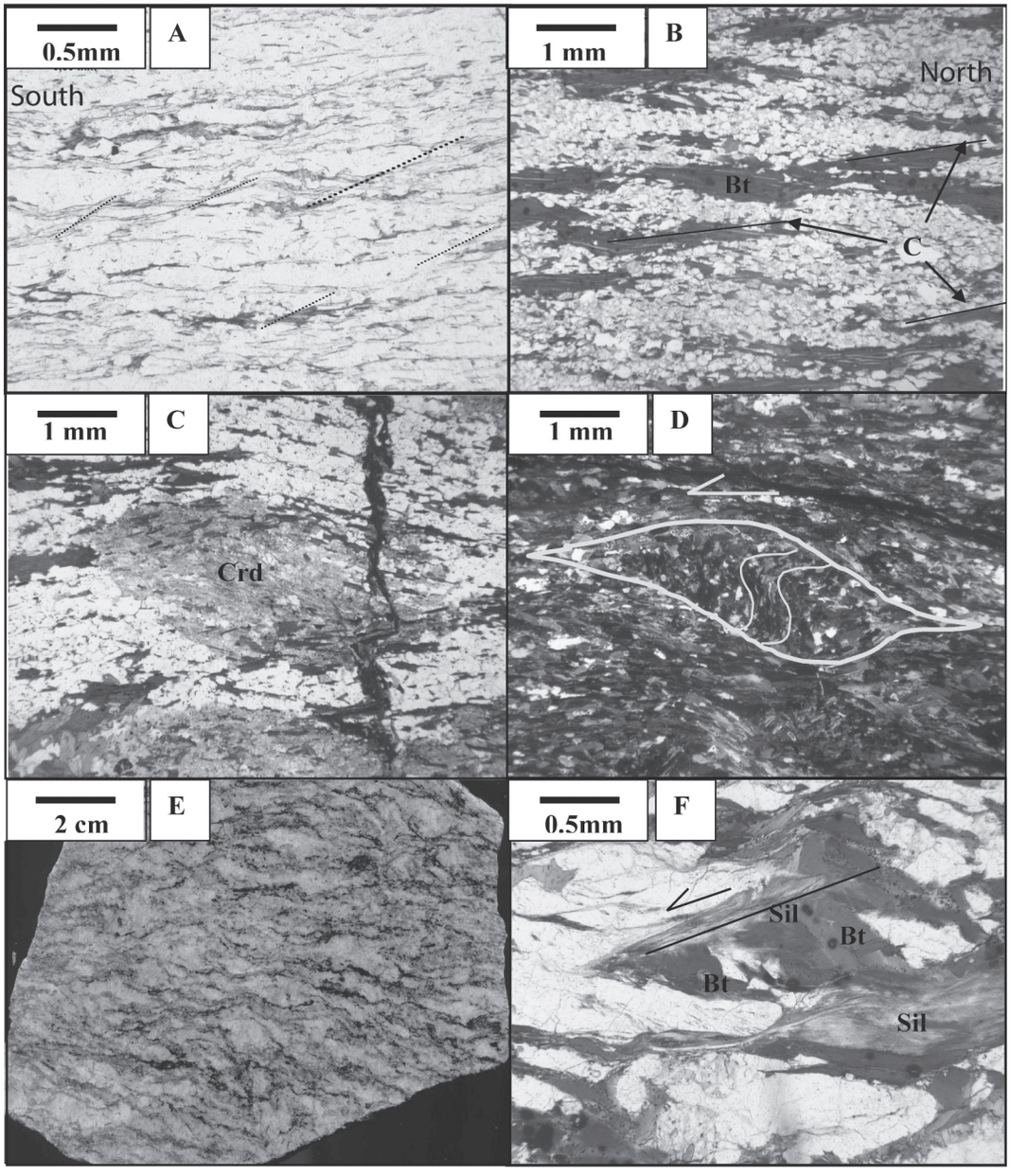

Fig. 5: Sil-Bt zone samples displaying top-to-the-south shear criteria, A and B are from Dompnac, C and D from Saint Laurent-les-Bains, and E and F from Le Sommet des Moles. N is on the right.
A: Quartzite sample (PLAR 70, see Fig. 4) where shear planes (thin black lines) cut the foliation with a high angle.

B: Pelite sample where biotites define the foliation with a sigmoid geometry (Bt) and are present in shear planes.

C: Natural-light view of a sigma shaped syntectonic cordierite (Crd).

D: Cross-polarized light view of shear-related folds in a sigmoid quartz-muscovite 'fish'.

E: X-Z section of an orthogneiss sample (between the dome and the MMVZ at SLB) showing evidence of normal shear.

F: Natural-light view of sillimanite bearing shear planes cross cutting magmatic biotite.

quartzite, though pre-anatectic schist in SLB displays some top-to-the-south normal shear sense critera such as C/S structures. At a microscopic scale, shear-sense criteria are still rare, and display when they exist top-to-the south normal shearing (Fig. 5).

In D, the proximity of the Rocles granite induces many granitic injections sub-parallel to the foliation (Fig. 4A). Closer to the Tanargue orthogneiss *in-situ* melting of the most pelitic layers is seen, suggesting that Rocles magma could result from the collection of anatectic liquids.

In SM as in SLB, the contact between the Sil-Bt zone and the dome is marked by mylonitic orthogneiss showing evidence (Sil-bearing shear planes, rotated KF clasts) of normal shear sense (Fig. 5E, F). Those orthogneiss are interpreted to represent the deformed equivalent of Rocles granite. Where the boundary between the MMVZ and the dome is E-W (western part), the Tanargue orthogneiss displays metric syn-anatectic folds with an E-W fold axes and a N-S stretching lineation (Fig. 4C: g) related to the dome emplacement.

The entire MMVZ is affected by retromorphic mesoscopic and microscopic shear planes. On the mesoscopic scale, steep (60-65° S) shear planes with striation in the dip, cut the ductile foliation and give normal sense of shear. On the microscopic scale, retromorphic Sil (Ms) and chloritic shear planes show nice C/S structures and a normal sense of shear (top-to-the south). The mesoscopic shear planes are difficult to relate to a precise event, whereas microscopic criteria (reflecting brittle-ductile normal shearing) is interpreted as being produced during a continuum of deformation, from ductile to brittle, durind the dome intrusion.. A 50m-thick cataclastic fault (pre-Triassic movement?) has reworked the whole MMVZ and has destroyed

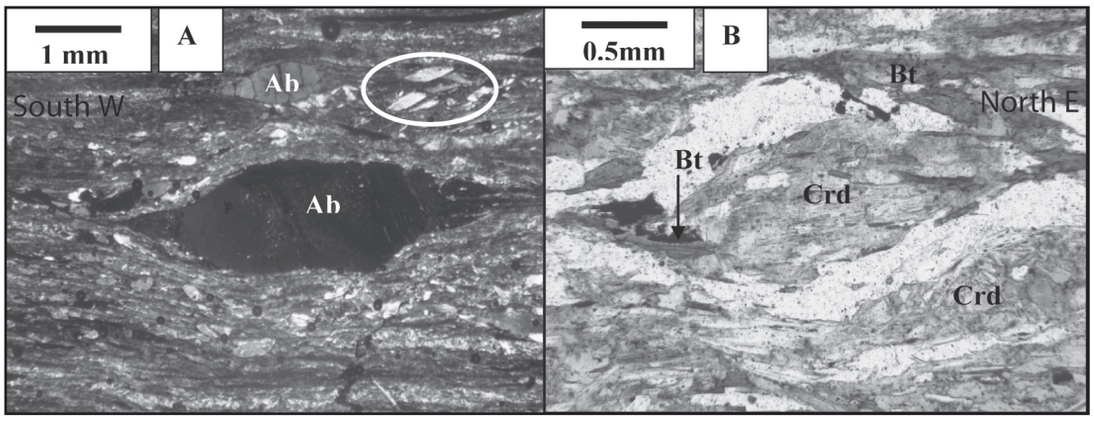

Fig. 6: Top-to-the-northeast shear criteria in Saint Laurent-les-Bains. Northeast is on the right. **A:** Cross-polarized-light view of mylonitic quartz-feldspar schist (PLAR 137) in greenschist facies of the southern-most part of the MMVZ. Sigmoïd albite (Ab) and a muscovite fish (in the circle) indicate top-to-the-northeast shearing. **B:** Sigmoid cordierite with biotite pressure shadows.

Fig. 7: Extreme folding of foliation in the And-Crd-Bt zone of Saint Laurent les Bains. The view is perpendicular to the stretching lineation.

the whole ductile foliation. This brittle fault juxtaposes the And-Crd-Bt zone against the Sil-Bt zone in SLB, the Sil-Bt zone against orthogneiss in SM, and the dome against the MMVZ in D (where the fault was sealed by highly siliceous fluids). Thus, this later brittle tectonic event cannot have caused the major apparent metamorphic gradient.

The andalusite-cordierite-biotite zone (i.e And-Crd-Bt zone)

*Dompnac cross section (*Fig. 4A*)*

From the south to the dome, Crd, And and Bt of Rocles metamorphic aureole show complex relationships with deformation. Sometimes the syn-deformational crystallization indicates top-to-the-east shearing. Static crystallizations can also be seen.

*Sommet des Moles cross section (*Fig. 4B*)*

Toward the dome, in the greenschist facies, some samples show deformation related to top-to-the-east shearing. Hornfels with a static crystallization of Bt and Crd could represent the Borne and/or the Rocles aureoles. Farther north in the Sill-Bt zone, these two minerals define a mylonitic foliation with a N200° 20° lineation composed of ellipsoidal biotitic agregates.

*St Laurent-les-Bains cross section (*Fig. 4C*)*

Spectacular relationships exist between the dome and the host schists. The mylonitic texture begins to appear in the greenschist facies, the south-dipping foliation is smoothly undulating, and mineral lineation is N240° 20° (Fig. 4C, a). In thin section, obvious criteria indicate top-to-the-northeast shearing (Fig. 6A), which means that a northeast thrust movement is a constant observation. Syntectonic Crd and Bt formed simultaneously, defining a well-developed mylonitic foliation and lineation oriented also N240° 20° (Fig. 4C, b). Top-to-the-northeast shearing, indicated by biotitic and cordieritic shear planes and sigmoid Crd (Fig. 6B), is widespread in the And-Crd-Bt zone. Small (cm- to dcm-scale) folds have an 'a' axis parallel to the lineation (Y-Z section: (Fig. 4C, c); their number increases in the metamorphic zone going toward the dome. In the X-Z section, folds again indicate top-to-northeast shearing. Just before crossing a large brittle fault, folding is widespread (Fig 4C, d; Fig. 7) and some Sil nodules formed from dactylitic Bt aggregates. Here, folds in X-Z and X-Y planes are contemporaneous and can be easily interpreted as created by constriction. In the Sil-Bt zone, new foliation was created by transposition and recrystallization of the previous (And-Crd-Bt zone) folded foliation. The Sil isograd may even be folded, in view of the fact that And > Sil reaction textures are observed over at least 20 m.

3.2.2 Quartz Crystal Preferred Orientation (C.P.O)

Crystallographic preferred orientations (CPO) of Qtz were measured by indexation of Electron Back-Scattered Diffraction (EBSD) patterns, using the JEOL JSM 5600 instrument of the Laboratoire de Tectonophysique at the University of Montpellier II. EBSD patterns are generated by the interaction of a vertical incident electron beam with a carefully polished sample inclined at 70° with respect to horizontal. Diffraction patterns are projected onto a phosphorus screen and captured by a low-light, high-resolution CCD camera. The image is then digitally processed and indexed in terms of mineral phase and crystal orientation, using CHANNEL+ software from HKL Technology. Measurements were made on a grain-by-grain basis and in operator-controlled indexing mode. Fabric strength was computed using Bunge's J index [38].

Four samples were analyzed. Three are from the Sil-Bt zone of D, SM and SLB – respectively PLAR 70, 192 (quartzite) and 182 (metapelite) – and the fourth is from the And-Crd-Bt zone of SLB (PLAR 22 quartzite).

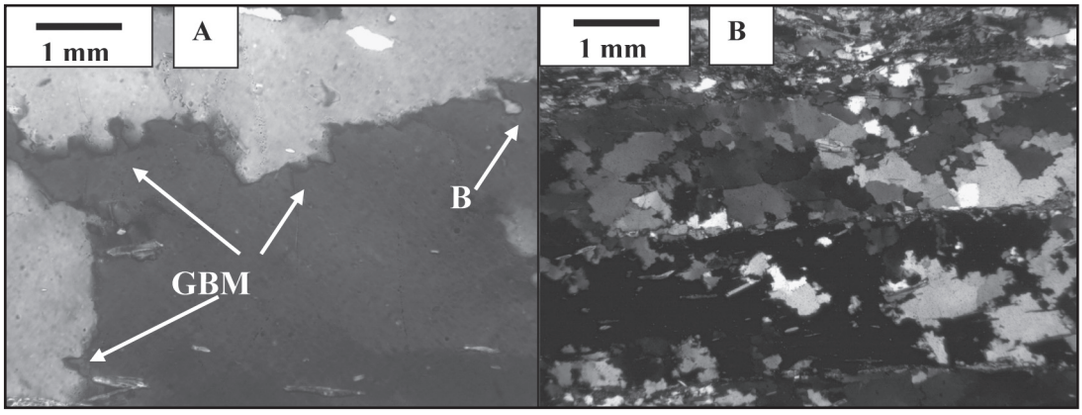

Fig. 8: Cross–polarized-light view of PLAR 70 showing foliation and quartz texture indicating important quartz grain boundary migration. **A:** Enlargement showing evidence of grain boundary migration (GBM) and bulging (B).

B: Overview of quartz band showing quartz amoeboïd texture.

Sillimanite zone samples

PLAR 70

The sample was collected close to the Sil+ isograde (Fig. 4A). The foliation is defined by Qtz-rich layers (Fig. 8) bounded by micas, mainly muscovite and rare biotite. Oriented Ms flakes included within large Qtz crystals define the foliation parallel to the layering. Qtz, the dominant phase, shows spectacular evidence of grain-boundary migration and bulging (Fig. 8). A minor amount of platen Qtz with straight, orthogonal boundaries is also present. This amoeboid Qtz texture (Fig. 8) is typical of high-temperature deformation.

Qtz CPO (Fig. 9) shows a well-developed high-temperature fabric; <a>, <m> and <c> axes have a strong point distribution that tends to mimic a single crystal, whereas <r> and <z> have a conical distribution without real point concentrations. The J index, which reflects fabric intensity, is 5.5 and is mostly due to the <c> axis concentration (pfJ=3.89) around the Y structural axes. The angle between <a> maximum and the X direction is quite large (39°) and is difficult to interpret in terms of top-to-the south shearing as suggested by the <a> maximum, as well as field- and thin-section observations.

PLAR 192 (Fig. 4B)

It is composed of Bt, Crd, Qtz, Sil and Kfs. Lineation (N240° 50°) is defined by Sil fibers. Foliation, rough at a mesoscopic scale, is strong in thin section where it is defined by layers of Qtz-Sil nodules (Fig. 10A). Some of these nodules have a sigmoid shape that provides a top-to-the-south sense of shear criteria (Fig. 10B). In these nodules, as inclusions, Sil defines the grain bouandery and defines shear planes providing the same top-to-the-south criteria. The foliation is sheared by retromorphic Ms bearing shear planes which also provide an apparent normal sense of shear.

Between the Qtz-Sil nodule layers, the matrix is composed of Qtz, feldspar and chloritized Bt. Most Qtz crystals are extinct in analyzed and polarized light. Some platen Qtz is elongated in the X direction and contributes to defining the general foliation trend. Qtz grains show evidence of bulging and grain-boundary migration, suggesting efficient diffusion and thus CPO is typical of prismatic <a> glide (Fig. 9), consistent with high-temperature deformation. This fabric shows a distribution of all the axes as a single Qtz crystal. But the most important point is that the distribution is symmetric to the foliation plane, and that the maximum of <a> axes indicates top-to-the-south shearing consistent with microstructures (sigmoid Qtz-sil nodules). J is very strong (J=8.08) and, as for PLAR 70, controlled by <c> axis concentration (pfJ=5.03), but strengthened by the other axes.

PLAR 182

This sample of anatectic metapelite was taken close to the dome (Fig. 4C,f). It is composed of Qtz, K-feldspar, acidic plagioclase, biotite, and Sil. In thin section, Sil defines the foliation (Fig. 11A) and bounds thin (0.5 mm) Qtz bands. Sil needles may be found within Qtz crystals, defining an internal fossil foliation concordant with the external one. The Sil bearing foliation is sometimes folded and indicates shear sense criteria which are not coherent (top-left; top-right). Feldspars show exsolution (perthite, and anti-perthite respectively) and mechanical twinning. Qtz displays evidence of large grain-boundary migration (Fig. 11B), especially bulging) and platen Qtz, suggesting sub-solidus high-temperature deformation. CPO agrees with high-temperature deformation accommodated by dominant prismatic <a> glide. The <c> axis (Fig. 9) is mostly concentrated on the finite Y deformation axis, but also defines a light girdle at 45° of the X axes. J remains moderate (J=3.74), due to girdle distribution of <m>, <c>, <r> and <z> axes. Furthermore, the <a> axes maximum could indicate a top-to-the-south normal sense of shear.

Andalusite-cordierite-biotite zone: PLAR 22

The sample was taken from the roof of the mylonite in the And-Crd-Bt zone, where all shear-sense criteria indicate a thrust movement to the northeast (Fig. 4C,c). The mylonitic foliation is defined by Qtz layers (Fig. 12A) separated by thin biotitic or cordieritic layers that are boudinaged and intersected by shear planes. The Qtz matrix is composed of rounded grains (<0.7 mm) that show evidence of dislocation creep, especially through strong wavy extinction (Fig. 12B). The porphyroclasts are commonly rimmed by smaller grains (Fig. 12B) interpreted as resulting from the dynamic recrystallization of porphyroclasts through sub-grain rotation. CPO shows a dominant rhomboidal slip system (Fig. 13) indicated by <c> axis maximum.

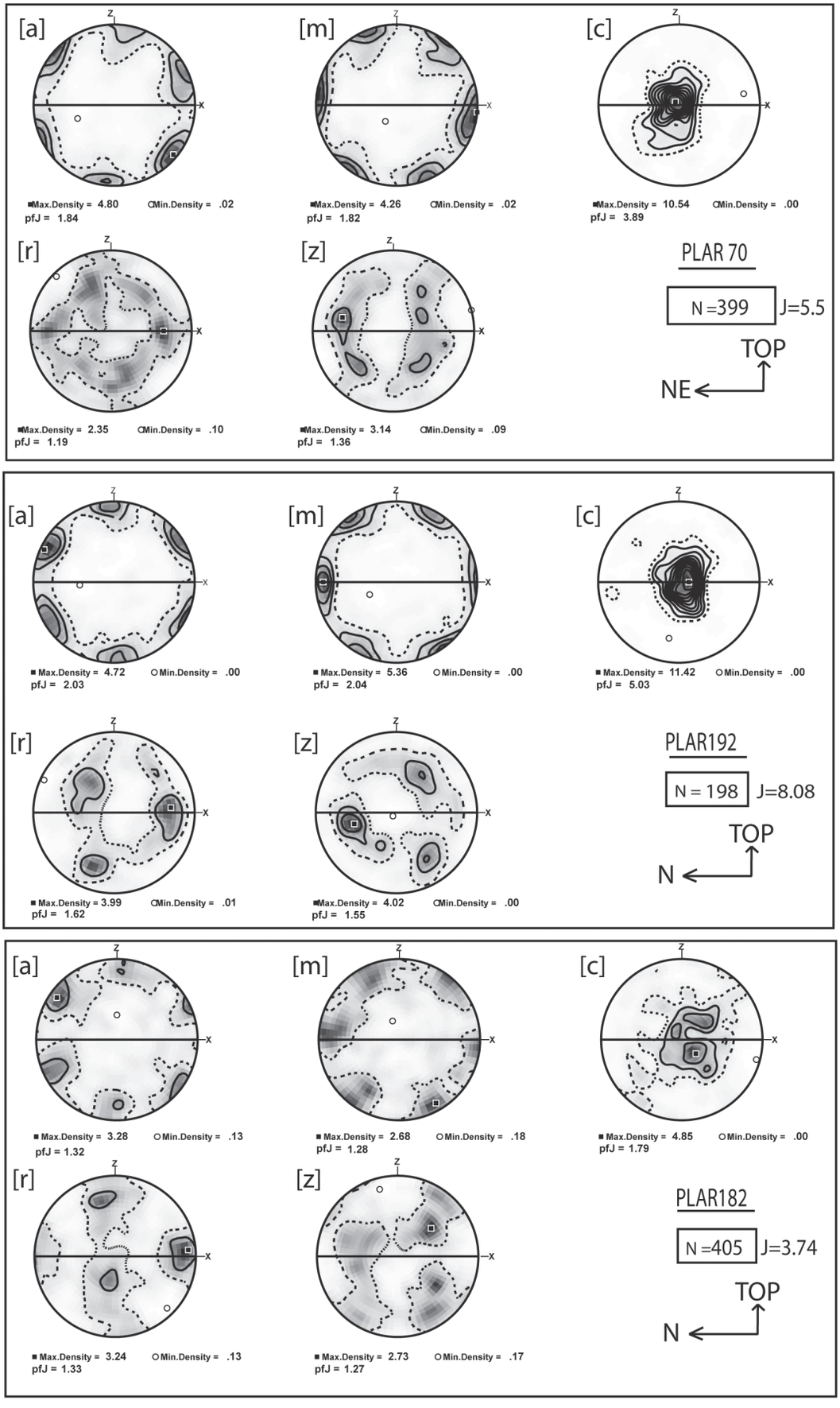

Fig. 9: Qtz CPO data of the Sil-Bt zone. N is number of measurements, J is Bunge's J index, and contours are each percent. Horizontal line is the foliation trace, and X and Z are the structural axes. For PLAR 192 Quartz-sillimanite nodules have not been analyzed.

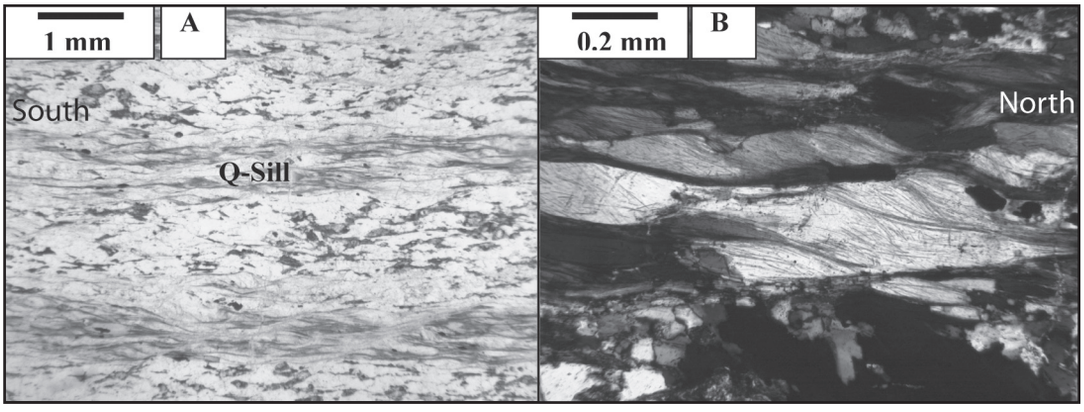

Fig. 10:
A: Natural-light view of the foliation of PLAR 192, marked by quartz-sillimanite nodule layers (Q-Sill). **B:** Nodules with a sigmoid shape indicate a ductile normal sense of shear. North is to the right.

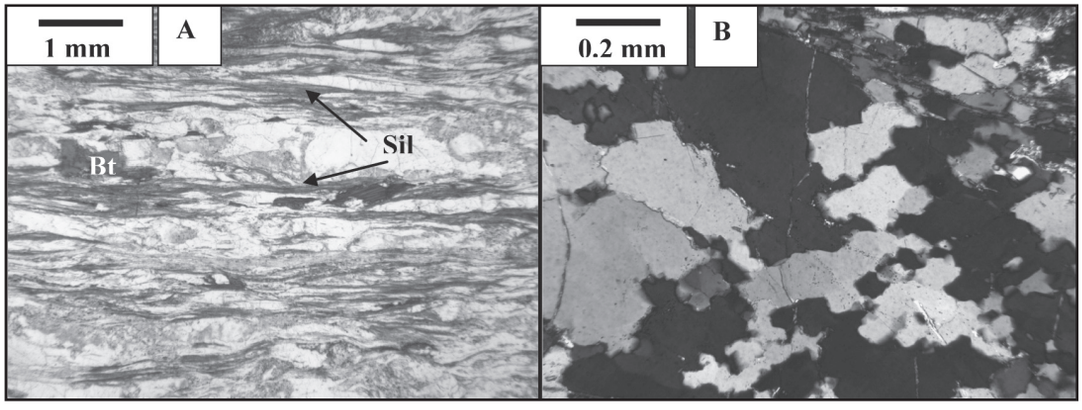

Fig. 11:
Sample PLAR 182.
A: Natural-light view of the mylonitic foliation marked by sillimanite (Sil) delimiting quartz-plagioclase bands. **B:** Cross-polarized-light view of quartz texture where grain boundary migration is important.

A dominant rhomboïdal slip system is consistent with MT-LP synkinematic metamorphic conditions. J is weak (J=2.86), due to the fact that the axes are generally distributed in a girdle. The asymmetry of the <a> maximum relative to the X axes suggests top-to-the-northeast shearing.

3.3. Timing of emplacement of the Velay dome

Deformation was contemporaneous with metamorphism; this means that, through $^{40}Ar/^{39}Ar$ determination on Bt and Ms, and U-Th-Pb on monazite, it is possible to constrain the timing of the last tectonometamorphic event that created the MMVZ. The following section uses criteria based on relative chronology, but also on absolute-age determination methods, to determine the timing of emplacement of the Velay dome.

$^{40}Ar/^{39}Ar$ thermochronology data were obtained in Montpellier by laser heating source extraction coupled to a mass spectrometer, on single Bt grains, and also by *in-situ* laser-probe analysis on polished thin sections (10*10*1 mm). Analytical procedure is described by Maurel *et al.* [39]. U-Th/Pb data were obtained on a single monazite grain, with a CAMECA SX 50 microprobe in the BRGM at Orleans; the method and procedure used is described by Cocherie and Albarede [40].

Relative emplacement time

Cobbles, consisting of paragneiss, mylonitic schist (the same paragenesis and mylonitic foliation as the MMVZ at SLB) and leucogranite from the dome were found in the basal conglomeratic deposits of the Carboniferous Prades-Jaujac basin (Fig. 3 [41]). Magmatic overgrowth of zircon in bentonite within the volcanoclastic rocks has been dated at 296 ± 6.8 Ma (U/Pb on Zr: [42]), indicating that the dome was already emplaced during Stephanian times. The Béssèges coal basin [43] (297.4 ± 4 Ma, U/Pb on Zr: [42]) lies behind the Borne massif, and its formation is related to the activity of eastward detachment, where meter-sized tectonic boudins of rocks from Borne aureole (dated at 310 ± 3 Ma [36]) have been found (Fig. 3). So the fourth tectonic episode (part 3.1) comtemporaneous with basin formation is characterized by E-W extension, and is post Borne granite emplacement, at around 300 Ma.

Absolute age determination

It has been carried out using two different methods on four samples located along the SLB cross section (Fig. 4C).

Determinations with the 40Ar/39Ar laser method:

PLAR 137 is a mylonitic greenschist-facies metapelite of the most external part of the MMVZ (Fig. 4C-a), where Ms 'fish' and sigmoid Ab crystals show clear top-to-the-northeast shearing (Fig. 6A). The Ms, dated by *in-situ* laser probe analysis, gives ages from 320 to 310 Ma, but one grain (Spot 6, *Table* 1) shows inherited values from the earlier Barrovian thickening event, documented in this region at 340 Ma [44, 45]. Considering that both Ms closure and deformation temperatures are around 450 °C, these ages can be considered as neocrystallization ages (e.g. [46]) during the

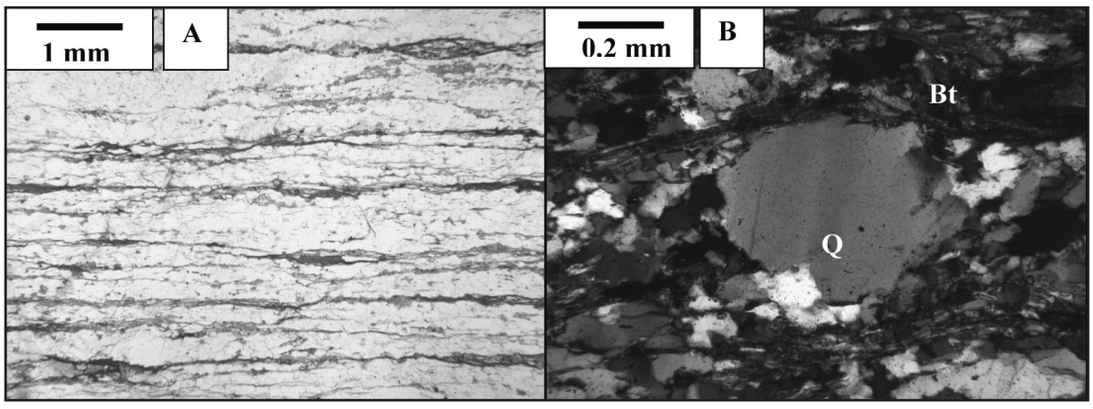

Fig. 12:
A: Natural-light view of the mylonitic foliation marked by syntectonic biotite of PLAR 22.
B: Cross-polarized-light view of quartz texture, where big crystals with wavy extinction and kink bands are rimmed by small new grains.

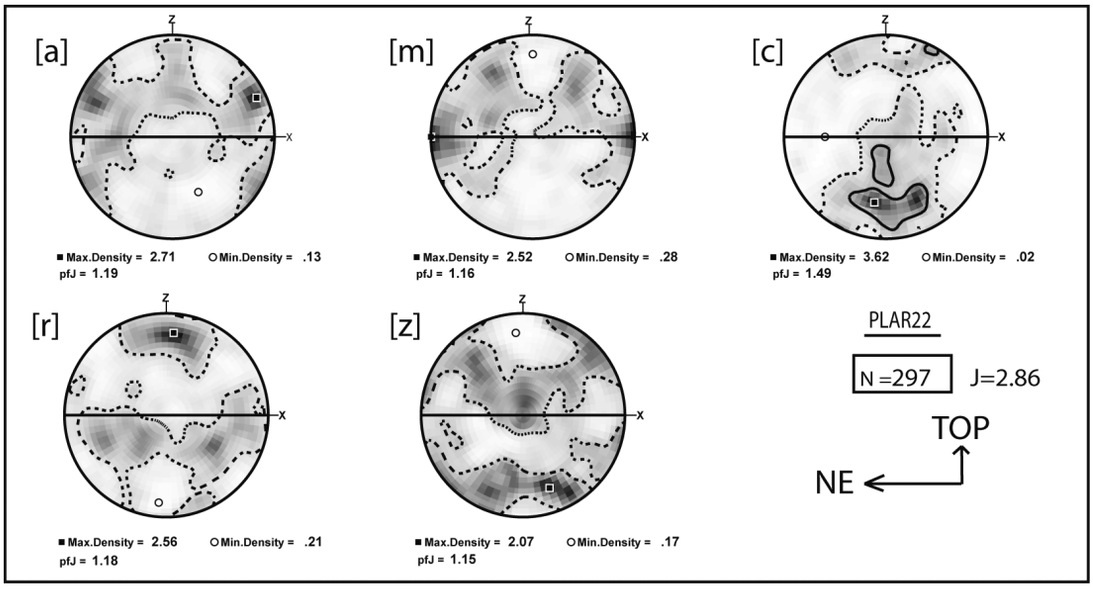

Fig.13: Qtz CPO data of PLAR 22, large and small grains have been analyzed and not differentiated in these patterns. N is number of measurements, J is Bunge's J index, contours are each percent. Horizontal line is the foliation trace and X and Z are the structural axes.

Table 1:
Ar/Ar ages on white micas from PLAR 137 using in-situ laser probe analysis.

pr137mus	40Ar*/39Ar x 1000	36Ar/40Ar	39Ar/40Ar	37Ar/39Ar	% 39Ar	% Atm,	Age	error
1	14,315	0,411	0,0613	0,019	4,8	12,1	315,22	1,87
2	14,11	0,062	0,0695	0,01	23,8	1,8	311,09	2,71
3	14,464	0,032	0,0683	0	55,5	0,9	318,23	2,36
4	14,464	0,107	0,0669	0	72,8	3,1	318,25	1,61
5	14,777	0,093	0,0657	0,019	79,4	2,7	324,54	2,22
6	15,89	0,064	0,0617	0	82,6	1,8	346,78	17,61
7	14,691	0,076	0,0665	0,013	100	2,2	322,81	4,26

northeastward shearing that occurred at least since 320 Ma, and which affected older micas.

PLAR 145 is a quartzite from the And-Crd-Bt zone of the MMVZ, where Bt marks the foliation and where all shear-sense criteria indicate northeastward shearing (Fig. 4C-b). The Bt blasts show a well defined plateau at 309.8 ± 3 Ma that correlates quite well with the total age of 309.3 ± 3 Ma (Fig. 14A). As the metamorphic assemblage indicates temperatures around 550 °C (using the P-T diagram of [47]; and Ti wt% in Bt) and assuming a closure temperature for Bt of around 350 °C, this age corresponds to cooling of the roof of the MMVZ (i.e.: And-Crd-Bt zone).

PLAR 148 is a granulitic paragneiss of the Sil-Bt (Ms-out without melt) zone, displaying top-to-the-south normal shearing (Fig. 4C). The age spectrum (Fig. 14B) shows a plateau age at 307 Ma, in agreement with the total age of 301 Ma. Two younger low-temperature steps are interpreted as a superficial loss of Ar by chloritization or weathering.

Determinations with the U-Th/Pb microprobe method:

Four monazite grains extracted from a metapelite leucosome (PLAR 182: Sil-Bt zone, Fig. 4C-f) located against the dome, have been analyzed. From electron microscopy images, we can see that two grains are homogeneous, and

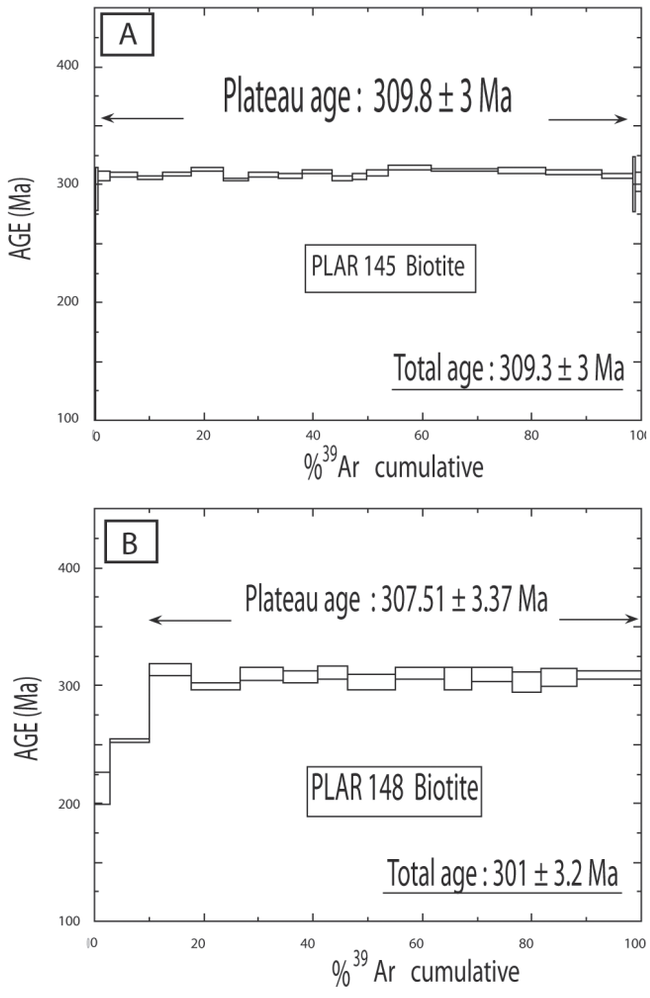

Fig. 14: A: Age spectra of a single biotite grain from PLAR 145 (And-Crd-Bt zone). **B:** Age spectra of a single biotite grain from PLAR 148, paragneiss of the Sil-Bt zone (Ms-Out).

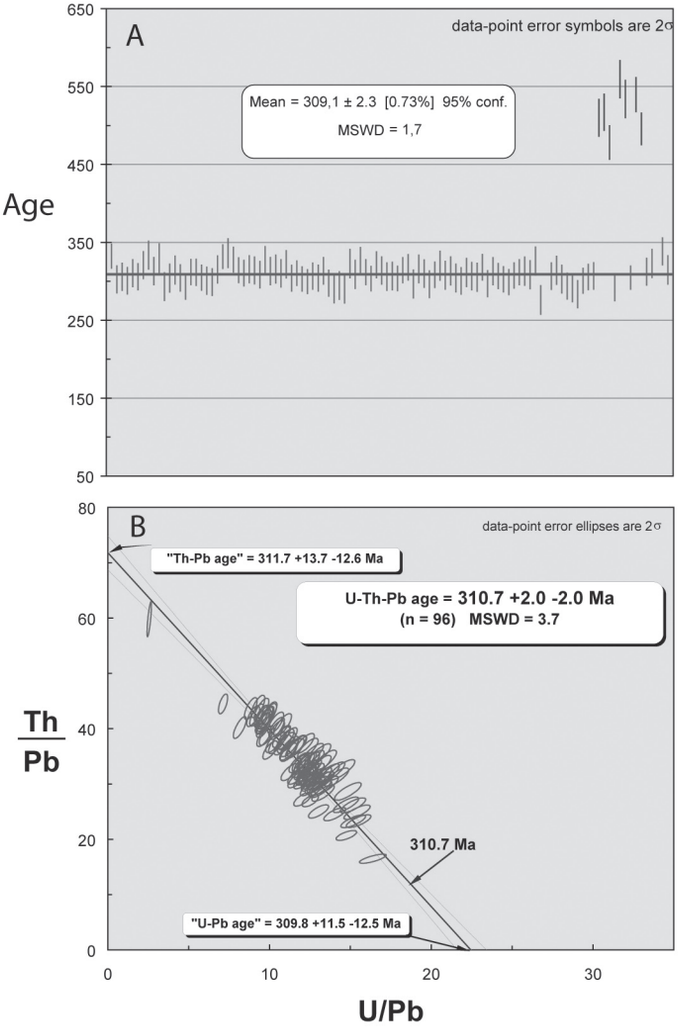

Fig. 15: A: Averaged age of all points from four monazite grains. Note the inherited component around 450 Ma corresponding to an inherited core.

B: U-Th/Pb regression line age obtained from the two homogeneous grains, the rim of the grains having an inherited core at 500 Ma, and all the analyses from the other heterogeneous grain. The age of 310 Ma is well defined by the regression line. The MSDW of 3.7 reflects mainly the fact that an age of around 330 Ma from the core of one of the heterogeneous grain has been included in the calculation.

give an age at 310 Ma (Fig. 15A). Two further grains are not homogeneous and show inherited values:

i. The first has an old inner core (500 Ma, Fig. 15A), interpreted as being a non-rehomogenized inherited sedimentary grain from metapelite, and a rim of around 310 Ma.

ii. The second has a core giving an age around 330 Ma and a rim of around 310 Ma. As the number of core analyses (10) was too small to provide a relevant age, we decided to include them in the calculation of the mean age regression line (Fig. 15B) obtained with rim-point and homogeneous grains analyses.

This calculation gives an age of 310.7 + 2 Ma (Fig. 15B). It corresponds to the closure temperature of monazite around 700 °C during cooling of the Vellave metamorphic migmatites. These data are consistent with earlier work on the migmatites, e.g. [48].

4. Discussion

(1) Throughout the Mylonitic Metamorphic Vellave Zone (MMVZ), foliation wrapped the dome shape. Mineral lineations in the Sil-Bt zone everywhere are perpendicular to the dome edge, and within the strong mylonitic foliation there are few shear-sense criteria that consistently indicate top-to-the-south normal shearing. Considering that Sil marks the mineral stretching lineation, and that the Qtz CPO suggests a dominant activation of the HT prismatic <a> slip system, the MMVZ is regarded as a high-temperature shear zone.

Although the three CPO data in the Sil-Bt zone are consistent with prismatic <a> creep, more detailed study of the orientation ellipsoid shows that two groups may be defined in a triangular plot of the P, R, G (Point, Random and Girdle) indexes calculated from the orientation-matrix eigenvalues (Fig. 16) (e.g. [49]). The <a> axes plot far from the P pole, close to the R-G joint. For PLAR 22 and 182, <a> plots in the R space, and for

PLAR 192 and 70 <a> plots in the G space. For the <c> axes we distinguish the same group of samples, but <c> axes from PLAR 22 and 182 plot in the middle of the R space, and those from PLAR 192 and 70 in the P space.

The two groups defined by using the P, G, R indexes are also distinguished in a Flinn-type diagram (Fig. 16). Moreover, PLAR 22 from the And-Crd-Bt zone stands out from the other samples from the Sil-Bt zone, its <a> and <c> axes plotting close to the K=1 line with almost the same values (respectively 0.6 and 0.8). The Sil-Bt zone samples have the same characteristics: <a> axes in the flattening field with very low K values (around 0), and <c> axes in the constriction field with K values significantly over 1 (2.1, 2.55 and 15). The plots suggest that there was a difference in the deformation regime between the And-Crd-Bt zone and the Sil-Bt zone, but also from east to west within the Sil-Bt zone. For the Sil-Bt zone, top-to-the-south normal shearing is indicated by some thin-section criteria and by <a> maximum of the CPO. Moreover, the high angles between <a> maximum and X (between 31° and 39°) and plots of the eigenvalues, are interpreted as representing a non-negligible pure-shear component in the deformation regime. The difference within the Sil-Bt zone from east to west is interpreted as a result of the overturning of the dome to the west, inducing a greater pure-shear component in the deformation regime.

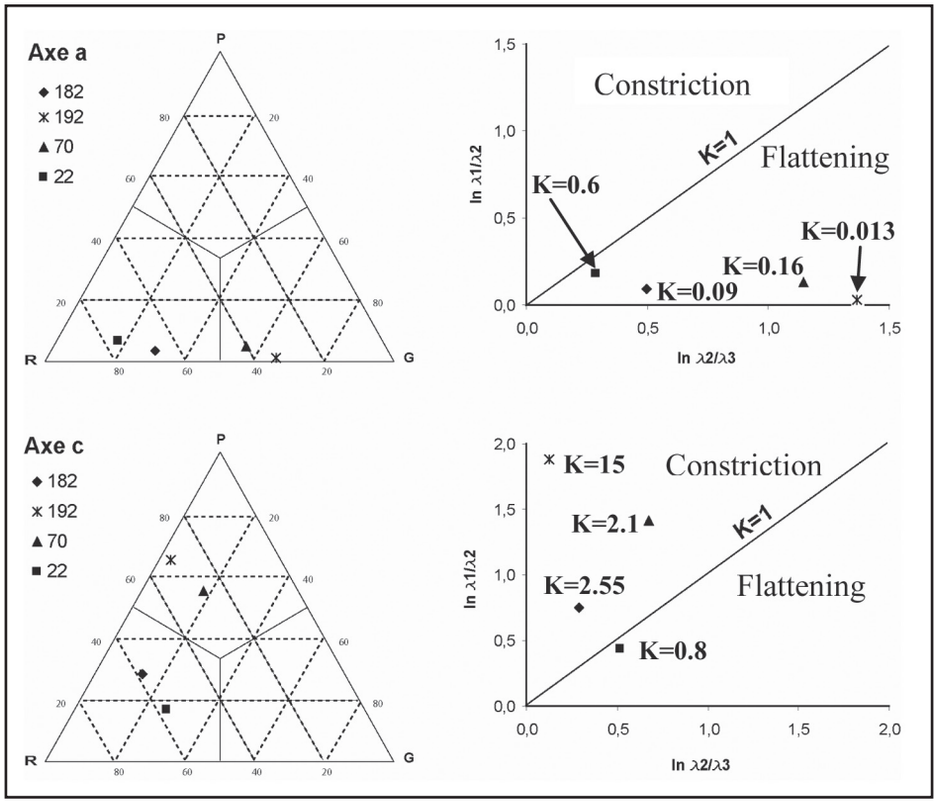

Fig.16: Triangular representation (P=point, R=random, G=girdle) of the eigenvalues of the <a> and <c>axes of the samples treated with EBSD. Next to each plot the Flinn type diagram of those axes, with their respective K values.

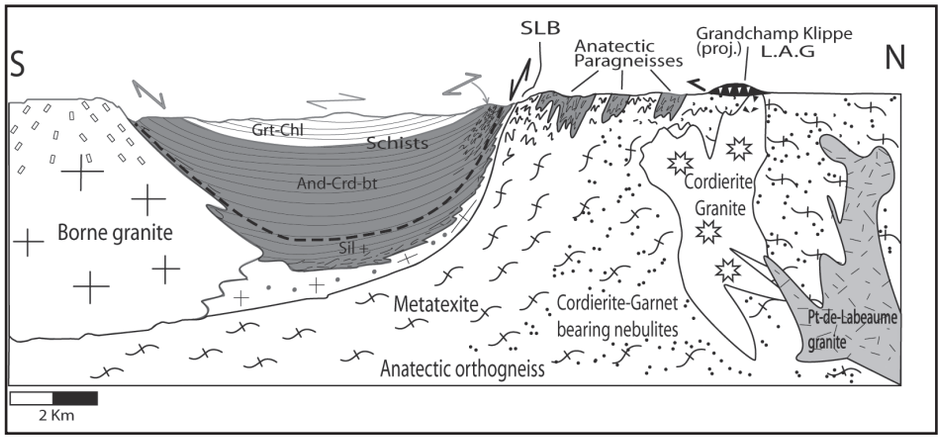

Fig.17: Crustal-scale cross section from the Borne granite edge to the southern rim of the Velay dome, passing through Saint Laurent-les-Bains. Thickness of the different units has been taken from [29], but this gravimetric model does not take account of the metamorphic grade of the series, so the incertainity is high for the schist thickness. Legend as in Fig. 4.

All these aspects lead to a non-negligible pure shear component in the deformation regime dominated by normal southward shearing; this interpretation is consistent with the presence of constriction observed in the And-Crd-Bt zone at SLB, and the extraordinary apparent metamorphic gradient. As a consequence, deformation in the Sil-Bt zone likely reflects the dynamics of the dome during its uplift and the intense shortening suffered by the Cévennes host rocks.

(2) Migmatization of the dome occurred at 314 ± 5 Ma [50], and our data from the MMVZ, monazite and biotite dating all fall around 310 Ma. In view of the closure temperatures of monazite and biotite, cooling of the dome from 700 °C to 350 °C took place in a short period, because the radiometric data of both chronometers are overlapping. This fast cooling implies that the migmatite body rose very fast (in 5 Ma or even less) and very high in the crust. The MMVZ follows the southern edge of the dome and is thus directly linked to the dome's emplacement as it, too, is dated at 310 Ma. It can

be assumed that the M3 episode of Montel *et al*. [11] (c.f : part 2.1.1) was responsible of the dome emplacement and the formation of the MMVZ, and not the M4 episode as earlier assumed (e.g. [22, 9]).

(3) As both the top-to-the-northeast shearing (well exposed in the western area of the highest structural level) and top-to-the-south shearing (observed in the Sil-Bt zone) are contemporaneous, two major hypotheses can be outlined with our data:

➤ The two opposite movements may be due to differential deformation between the dome and the host rock during uplift. Experimental models (e.g. [51]), but also field observations (e.g. Lévézou dome in the French Massif Central [52]) are well interpreted in terms of opposite shearing in a single diapiric event.

➤ Top-to-the-northeast shearing, active since at least 320 Ma as indicated by white-mica dating, is recorded in the highest structural terranes, from the dome until the contact aureole of Borne granite. Earlier works on the southern part of the dome also relates a northward movement [53, 23, 6, 7]. Consequently, this northeastward shearing was a regional tectonic event during dome initiation, affecting the medium to upper crust. This event, characterizes the tectonic framework of the late evolutionary stage of the Variscan belt in the French Massif Central (e.g. [14, 15]). So, in the same tectono-metamorphic event, a top-to-the-north flat detachment (Pilat?) fault system, active since 320 Ma, has been tilted to the south during the rapid dome emplacement, while this detachment was still active.

5. Conclusions

Detachment fault is a common feature of metamorphic core complex. The emplacement of MCC has been studied through this typical structure. In the case of the Massif Central, the Montagne Noire dome emplacement has been well constrain by the study of its detachment which highlighted the key role of its detachment fault (e.g [18]). In the case of the Velay dome, only the works of Lagarde [6] [7] and Dupraz [5] have shown a global model for its emplacement. They highlight the fact that the dome, during its emplacement assisted by its detachment fault on the northern side (the Pilat fault) has expanded toward the south. The fact that klippes on this detachment fault are found on the roof of the dome, show that the dome has intruded its own detachment. The characteristics of the Velay dome to intrude its own detachment is shown here on its southern edge.The Sil-Bt zone represents the uplift dynamics of the dome in the Cévennes host rock. It is characterized by a deformation with a great amount of pure shear and a normal sense of shear (top-to-the south) for its simple shear component. The klippe of greenschist facies terranes, which crops out between Borne granite and the dome, affected by constant the top-to-the-northeast shearing (from at least 320 Ma onward), is interpreted as representative here of the detachment fault. In this meaning, the And-Crd-Bt zone of St Laurent-les-Bains shows the interaction of the dome dynamics and the tectonic framework of the middle to upper crust (Fig. 17). This zone was tightly folded through constriction, sandwiched between the upper zone dominated by the detachment tectonics, and the Sil zone linked to the dome emplacement. As all thermochronometers used are set at 310 Ma, the MMVZ cooled very fast, suggesting rapid emplacement high in the crust. Southward, no evidence of this detachment has been observed, suggesting that Borne granite intrudes it, as the dome did, participating to the formation of this detachment klippe (Fig. 17).

Acknowledgments

We are grateful to the B.R.G.M. for funding this study. Special thanks go to the Université Montpellier II Geochemistry team for support and to Rémi Enjolvy for his help in monazite datation.

References

[1] Davis G.H. and Coney P.J., Geologic development of Cordilleran metamorphic core complex, Geology 7 (1979) 120-125.

[2] Lister G., Davis G.A., The origin of metamorphic core complexes and detachment faults formed during Tertiary continental extension in the northern Colorado River region, USA, J. of Struct. Geol. 11 (1989) 65-94.

[3] Vanderhaeghe O., Burg J.P., Teyssier C., Exhumation of migmatites in two collapsed orogens: Canadian cordillera and French variscides, Geological Society of London Special Publication 154 (1999) 181-204.

[4] Malavieille J., Guihot P., Costa S., Lardeaux J.M., Gardien V., Collapse of the thickened Variscan crust in the French Massif Central: Mont Pilat extensional shear zone and St. Etienne Late Carboniferous basin, Tectonophysics, 177 (1990) 139-149.

[5] Dupraz J., Didier J., Le complexe anatectique du Velay (MCF) : structure d'ensemble et évolution géologique, Géol. de la France 4 (1988) 73-88.

[6] Lagarde J.L., Dallain C., Capdevilla R., Contexte tectonique de la fusion crustale post collision dans la chaîne Hercynienne : l'exemple du complexe anatectique du Velay, C. R. Acad. Sc. 311 (1990) 477-484.

[7] Lagarde J.L., Dallain C., Ledru P., Courrioux G., Strain patterns within the late Variscan granitic dome of Velay (MCF), J. of Struct. Geol., 16-6 (1994) 839-852.

[8] Burg J.P., Vanderhaeghe O., Structures and way-up criteria in migmatites, with application to the Velay Dome (MCF), J. of Struct. Geol. 15-11 (1993) 1293.

[9] Ledru P., Courrioux G., Dallain C., Lardeaux J.M, Montel J.M., Vanderhaeghe O., Vitel G., The Velay dôme: melt generation and granite emplacement during orogenic evolution, Tectonophysics 342 (2001), 207-237.

[10] Montel J.M., Weber C., Barbey P., Pichavant M., Thermobarométrie du domaine anatectique du Velay (MCF) et conditions de genèse des granites tardi-migmatitiques, C. R. Acad. Sc. 302-9 (1986) 647-652.

[11] Montel J.M., Marignac C., Barbey P., Pichavant M., Thermobarometry and granite genesis: the Hercynian low-P high-T Velay anatectic dome, J. Metam. Geol. 10 (1992) 1-15.

[12] Kretz, R., Symbols for rock-forming minerals. American Mineralogist, 68 (1983) 277–279.

[13] Matte P., Tectonics and plate tectonics model for the Variscan Belt of Europe, Tectonophysics 126 (1986) 329-274.

[14] Matte P., Accretionary history and crustal evolution of the Variscan Belt in Western Europe, Tectonophysics 196 (1991) 309-337.

[15] Faure M., Leloix C., Roig J.Y., L'évolution polycyclique de la chaîne hercynienne, Bull. Soc. Géol. France 168-6 (1997) 695.

[16] Burg J.P., Van den Driessche J., Brun J.P., Syn-Thickening to Post-Thickenning extension, mode and consequences, C. R. Acad. Sc. 319-9 (1994) 1019-1032

[17] Leyreloup A.F., La croûte métamorphique du sud de la France – Géologie de surface et des enclaves remontées par les volcans Cénozoïques, Doctorat d'état, Thesis University of Montpellier II, 1992.

[18] Van den Driessche J., Brun J.P., Tectonic evolution of the Montagne Noire – a model of extensional gneiss dome, Geodinamica Acta 1-2 (1992) 85-99.

[19] Quenardel J.M., Santallier D., Burg J.P., Bril H., Cathelineau M., Marignac S., Le Massif Central, Bull. Soc. Geol. France 44-4 (1991) 163-179.

[20] Gardien V., Lardeaux J.M., Découverte d'éclogites dans le synforme de Maclas : extension de l'unité supérieure des gneiss à l'Est du MCF, C.R.Acad. Sc., 312 (1991) 61.

[21] Gardien V., High to medium pressure relics in the eastern Vivarais series (eastern part of the Massif Central), C. R. Acad. Sc. 316 (9) (1993) 1247-1254.

[22] Barbey P., Marignac C., Montel J.M., Macaudiere J., Gasquet D., Jabbori J., Cordierite growth textures and the conditions of genesis and emplacement of crustal granitic magmas: the Velay granite complex, J. of Petrology 10-9 (1999) 1425-1441

[23] Macaudière J., Barbey P., Jabbori J., Marignac C., Le stade de la fusion initiale dans le développement des dômes anatectiques : le dôme du Velay (MCF), C. R. Acad. Sc. 315 (1992) 1761.

[24] Guérangé-Lozes J., Burg J.-P., Les nappes varisques du sud-ouest du Massif central: Cartes géologiques et structurales à 1/250 000 Montpellier et Aurillac. Bulletin du B.R.G.M., série "Géologie de la France", 3-4 (1990) 71-106.

[25] Arnaud F., Boullier A.M., Burg J.P., Shear structures and microstructures in micashists: the Variscan Cévennes Duplex (MCF), J. of Struct. Geol. 26 (2004) 588-868.

[26] Rakib A., Le métamophisme régional de basse pression des Cévennes occidentales : une conséquence directe de la mise en place du dôme thermique vellave (MCF), Doctorat, Thesis University of Montpellier II, 1996.

[27] Marignac C., Leroy J., Macaudiere J., Pichavant M., Weisbrod A., Evolution tectonométamorphique d'un segment de l'Orogène Hercynien : les Cévennes médianes, C. R. Acad. Sc. 291 (1980) 605-609.

[28] Faure M., Charonnat X., Chauvet A., Schéma structural et évolution tectonique du domaine para-autochtone cévenol de la Chaîne Hercynienne, C. R. Acad. Sc., 328 (1999) 401-407.

[29] Faure M., Charonnat X., Chauvet A., Chen Y., Talbot J.Y., Martelet G., Courrioux G., Monié P., Milesi J.P., Tectonic evolution of the Cévennes para autochthonous domain of the Hercynian French MC and its bearing on ore deposits formation, Bull. Soc. Geol. France 172-6 (2001) 687-696.

[30] Weisbrod A., Explication sommaire de la carte géologique des Cévennes médianes, Sciences de la terre 12-4 (1969) 301-344.

[31] Mialhe J., Le massif granitique de la Borne, étude petrographique, géochimique et géochronologique, doctrat d'état, Thesis 1980.

[32] Be Mezeme E., Faure M., Chen Y., Cocherie A., Talbot J.Y., Structural, AMS and geochronological study of a laccolith emplaced during Late Variscan Orogenic extension: The Rocles Pluton (SE Massif Central), submitted to inter. J. of Earth Sciences.

[33] Grambling J.A., Internally-consistent geothermometry and H_20 barometry in metamorphic rocks: example garnet-chlorite-quartz, Contrib. Miner. Petr. 105 (1990) 617.

[34] Toteu F., Utilisation des analyses chimico-minéralogiques et microstructurales dans la reconstitution des évènements tectonométamorphiques des formations polycycliques, Doctorat, Thesis Nancy, 1981.

[35] Lacassin R., Van Den Driessche J., Analyse de la déformation hercynienne majeure des gneiss de la Cézarenque, C. R. Acad. Sc., 295 (1982) 1027-1030.

[36] Monie P., Respaut J.P., Brichaud S., Bouchot V., Faure M., Roig J.Y., $^{40}Ar/^{39}Ar$ and U-Pb geochronology applied to Au-W-Sb metallogenesis in the Cévennes and Chataigneraie districts (southern Massif Central, France), BRGM Documents 297 (2000) 77-79.

[37] Talbot J.Y., Chen Y., Faure M., Lin W., AMS study of the Pont de Montvert-Borne porphyritic granite pluton (MCF) and its tectonic implications, Geophys. J. Int. 140 (2000) 677-686.

[38] Bunge H.J., Texture Analysis in Materials Sciences, Buttleworth, London, 1982, 593 pp.

[39] Maurel O., Monié P., Respaut JP, Leyreloup A.F, Maluski H., Pre-metamorphic $^{40}Ar/^{39}Ar$ and U-Pb ages in HP metagranitoids from the Hercynian Belt (France), Chemical geology 193-3-4 (2003) 195-214.

[40] Cocherie A., Albarède F., An improved U-Th/Pb age calculation for electron microprobe dating of monazite, Geochimica et Cosmochimica Acta 65 (24) (2001) 4509-4522.

[41] Lapadu Hargues P., Etude du bassin houiller de Prades, DES de Sciences Naturelles, 1 (1939), 22p.

[42] Brugier O., Becq-Giraudon J.F., Champenois M., Deloule E., Ludden J., Mangin D., Application of zircon geochronology and accessory phase chemistry to constraining basin development during post-collisional extension: a case study from the French Massif Central, Chemical Geology 201 (2003) 319-336.

[43] Allemand P., Lardeaux J.M., Dromart G., Ader M., Extension tardi-orogenique et formation des bassins intracontinentaux : le bassin stéphanien des Cévennes, Geodinamica Acta 10-2 (1997) 70-80.

[44] Caron, C., 1994. Les minéralisations Pb-Zn associées au Paléozoïque inférieur d'Europe méridionale. Traçage isotopique Pb-Pb des gîtes de l'Iglesiente (SW Sardaigne) et des Cévennes et évolution du socle encaissant par la géochronologie U-Pb, ^{40}Ar-^{39}Ar et K-Ar. Doctorat Thesis, University of Montpellier II.

[45] Cocherie A., Be Mezeme E., Legendre O., Mark Fanning C., Faure M., Rossi P., Electron microprobe dating as a tool for determining the closure of U-Th/Pb systems in migmatitic monazites, American Mineralogist, 90 (2005) 607-618.

[46] Dunlap W.J., Neocrystallisation or cooling? $^{40}Ar/^{39}Ar$ ages of white micas from low-grade mylonites, Chemical Geology 143 (1997) 181-203.

[47] Tinkam K.D., Zuluaga C.A., Stowell H.H:, Metapelite phase equilibria modeling in MnNCKFMASH: the effect of variable Al_2O_3 and MgO/(MgO+FeO) on mineral stability, Geological Material Research 3-1 (2001)..

[48] Be Mezeme E., Faure M., Cocherie A., Chen Y., In situ chemical dating of tectonothermal events in the French Massif Central, Terra Nova 00 (2005) 1-7.

[49] Mauler A., Godard G., Kunze K., Crystallographic fabrics of omphacite, rutile and quartz in Vendée eclogites (Armorican Massif, France). Consequences for deformation mechanisms and regimes, Tectonophysics 342 (2001) 81–112.

[50] Mougeot R., Respaut J.P., Ledru P., Marignac C., U-Pb chronology on accessory minerals of the Velay anatectic dome, Eur. J. Mineral. 9 (1997) 141-156.

[51] Dixon, J.M., Finite strain and progressive deformation in models of diapiric structures, Tectonophysics 28 (1975) 89-124.

[52] Burg J.P., Regional shear variation in relation to diapirism and folding, J. of Struct. Geol. 9-8 (1987) 925.

[53] Laumonier B., Marignac C., Cheilletz A., Macaudiere J., Relation entre tectonique superposées,migmatisations et mise en place des granites sur l'exemple de la bordure sud du dôme du Velay, C. R. Acad. Sc., 313 (1991) 937-944.